ARMY RESEARCH LABORATORY

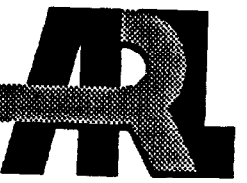

A Single-Stage Reconnection Gun

C. R. Hummer
C. E. Hollandsworth

ARL-TR-14

November 1992

NOTICES

Destroy this report when it is no longer needed. DO NOT return it to the originator.

Additional copies of this report may be obtained from the National Technical Information Service, U.S. Department of Commerce, 5285 Port Royal Road, Springfield, VA 22161.

The findings of this report are not to be construed as an official Department of the Army position, unless so designated by other authorized documents.

The use of trade names or manufacturers' names in this report does not constitute indorsement of any commercial product.

REPORT DOCUMENTATION PAGE

Form Approved
OMB No. 0704-0188

1. AGENCY USE ONLY *(Leave blank)*	2. REPORT DATE	3. REPORT TYPE AND DATES COVERED
	November 1992	Final, March 1990–June 1991

4. TITLE AND SUBTITLE

A Single-Stage Reconnection Gun

5. FUNDING NUMBERS

PE: 62618A
PR: 1L162618AH80

6. AUTHOR(S)

C. R. Hummer and C. E. Hollandsworth

7. PERFORMING ORGANIZATION NAME(S) AND ADDRESS(ES)

8. PERFORMING ORGANIZATION REPORT NUMBER

9. SPONSORING/MONITORING AGENCY NAME(S) AND ADDRESS(ES)

U.S. Army Research Laboratory
ATTN: AMSRL-OP-CI-B (Tech Lib)
Aberdeen Proving Ground, MD 21005-5066

10. SPONSORING/MONITORING AGENCY REPORT NUMBER

ARL-TR-14

11. SUPPLEMENTARY NOTES

12a. DISTRIBUTION/AVAILABILITY STATEMENT

Approved for public release; distribution is unlimited.

12b. DISTRIBUTION CODE

13. ABSTRACT *(Maximum 200 words)*

A magnetic coil with a square air core was constructed to launch metal plates in the edge-on orientation. The interaction between the magnetic field produced by a current through the coil and the induced currents in the plate accelerates the plate in a direction parallel to its plane. This induction launcher, called a reconnection gun, was used to launch a variety of aluminum, copper, and iron plates of varying thicknesses. The maximum velocity achieved was 250 m/s for a 96-g aluminum plate.

An equation of motion for the plate was derived from the total energy of the reconnection gun circuit and the kinetic energy of the plate. Final velocities from this equation of motion are within an error range of –0.09 to +0.21 of the measured velocities for a wide variety of experimental conditions. This equation is being used to help design another reconnection gun to launch heavier plates to higher velocities.

14. SUBJECT TERMS	15. NUMBER OF PAGES
launchers, magnetic fields	40
	16. PRICE CODE

17. SECURITY CLASSIFICATION OF REPORT	18. SECURITY CLASSIFICATION OF THIS PAGE	19. SECURITY CLASSIFICATION OF ABSTRACT	20. LIMITATION OF ABSTRACT
UNCLASSIFIED	UNCLASSIFIED	UNCLASSIFIED	UL

INTENTIONALLY LEFT BLANK.

TABLE OF CONTENTS

INTENTIONALLY LEFT BLANK.

LIST OF FIGURES

INTENTIONALLY LEFT BLANK.

LIST OF TABLES

INTENTIONALLY LEFT BLANK.

ACKNOWLEDGMENTS

The authors wish to give special thanks to Mr. C. Stumpfel for the infrared photographs of the plates. Mr. J. Correri prepared the facilities for the capacitor bank and Mr. K. Mahan helped construct the launch coil. Mr. A. Zielenski provided the capacitor bank, the power supply, and helpful suggestions. Dr. D. Hackbarth commented on the report.

INTENTIONALLY LEFT BLANK.

1. INTRODUCTION

Investigations into active protection systems have renewed interest in the interaction between flying plates and moving rods. Previous work in this area concentrated exclusively on interactions where the velocity vector of an explosively launched plate was normal to the plane of the plate (Frey, Melani, and Stegall 1988). Based upon simulations with the computer code HULL, it was suggested (Prakash 1990) that it would be advantageous to have the velocity of the plate parallel to the plane of the plate. Preliminary validation experiments (Thomson et al. 1991) tend to support this idea. Because of the difficulties in using explosive charges to launch a plate with this orientation, an alternate method is desirable.

The reconnection gun, invented (Cowan 1987) and developed (Cowan et al. 1986) at Sandia National Laboratories (SNLA), Albuquerque, NM, provides an attractive option for plate launch in the edge-on orientation. The reconnection gun induces a current in the plate by a time varying magnetic field produced by an external launch coil. This is similar to the action of a transformer where the primary winding, the external launch coil, induces a current in the secondary winding, the plate. The force between the magnetic field and the induced current in the plate accelerates the plate. This type of electromagnetic launcher has no electrical contact with the plate, and it has a relatively high efficiency for masses greater than a few hundred grams.

The group at SNLA built a multistage reconnection gun (Cowan et al. 1988) to accelerate an aluminum plate to high velocities. By properly timing the pulsed power delivered to successive acceleration stages, a 150-g aluminum plate was launched at a velocity of 1 km/s. Although the use of a multistage reconnection gun obviates the need for high explosives, its use in active protection systems may not be practical because of its size and weight. Therefore, a single-stage reconnection gun is considered here.

A single-stage reconnection gun (Hummer and Hollandsworth 1991) consisting of a square helical coil connected to a 11-kV, 100-kJ capacitor bank was constructed and used to accelerate, in the edge-on orientation, a number of rectangular plates of aluminum, iron, and copper whose masses ranged from 96 g to 631 g. The final velocities of the plates were measured with break-wire arrays and compared to the predictions of an equation of motion

derived from the total energy of the electrical circuit and the kinetic energy of the plate. This equation of motion was further tested by comparing the predicted velocity of an aluminum plate, as it was being launched, to experimental results. The position of this aluminum plate was detected by an optical system during launch, and its velocity was then determined from these data.

In an auxiliary experiment, an infrared image of an aluminum plate was taken just after it was launched. This image showed that the back edge and the sides of the plate were heated during the launch. This method could be used to find the temperature distribution and an average current density distribution in the plate. These data are valuable in studying qualitatively the magnetic field distribution in the coil and plate.

2. EQUATION OF MOTION

The equation of motion can be used to predict the performance of any proposed design of a reconnection gun. Once the capacitance, the equivalent resistance, and the inductance gradient of the launch coil are given for a particular design, then the velocity and the position of the plate and the circuit current can be estimated at any time. It can also be used to estimate the velocity and the position of the plate during the actual launching by a reconnection gun, once the inductance gradient of the launch coil is known and the circuit current is measured.

The equation of motion is complicated by the dependence of the inductance of the launch coil L (x(t)) on the position of the plate x(t) within the coil. This is caused by the distortion of the magnetic field in the coil. As an example, assume that the back edge of the plate is positioned close to the back side of the coil. When current flow establishes a magnetic field within the coil, the field lines that are normally parallel to the coil axis are bent around the perimeter of the plate and concentrated in the narrow gap between the plate and the back side of the coil by the induced current in the plate. This distortion of the magnetic field is illustrated in Figure 1 by a two-dimensional calculation.

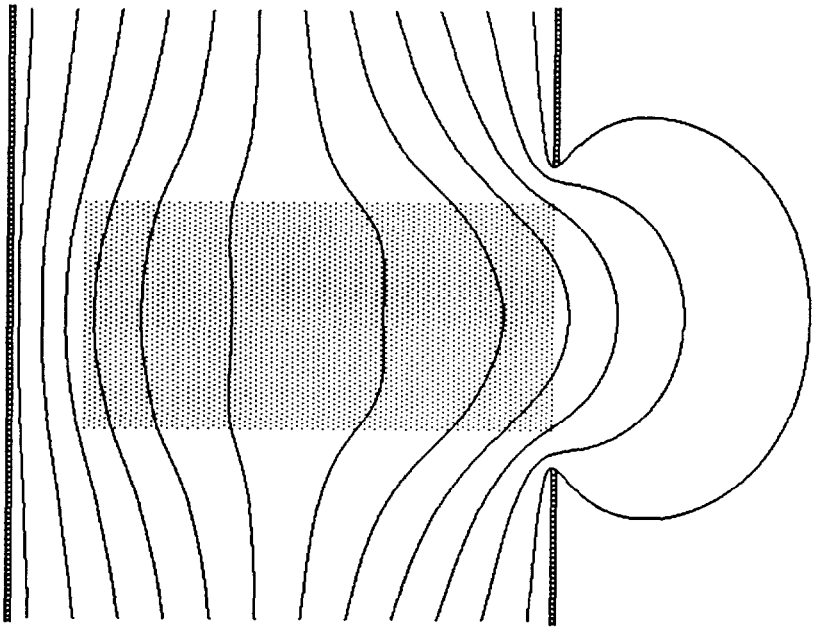

Figure 1. Magnetic Stream Lines Around an Aluminum Plate in an Oscillating Magnetic Field.

The shaded area in Figure 1 represents an aluminum plate in an oscillating magnetic field produced by two infinite current sheets. The current sheets are located at the hatched lines to the left and to the right of the aluminum plate, and they are perpendicular to the page. The current in these sheets are equal and opposite at all times. If the current in the sheet to the left of the aluminum plate is directed out of the page, then there is an equal current in the sheets to the right directed into the page. The lines between the current sheets are the stream lines for the magnetic field. The direction of the magnetic field is tangent to the lines, and the magnitude is inversely proportional to the distance between neighboring lines. Thus, the concentration of the field lines in the gap between the edge of the plate and the left current sheet represents an area where the magnitude of the magnetic field is large. The interaction of the large magnetic field in the gap and the induced current in the plate pushes

the plate through the slot in the current sheets to the right and out of the coil. As the plate is being pushed out of the coil, the shape of the magnetic field lines change which in turn changes the inductance of the coil.

To derive the equation of motion of the plate, it is assumed that the electrical circuit for a single-stage reconnection gun consists of a capacitor, a resistor, and a time-varying inductor all connected in series (Figure 2). The total energy of this system,

$$E(t) = Q^2(t)/2C + L[x(t)]\, I^2(t)/2 + m\, v^2(t)/2 \ , \qquad (1)$$

is the sum of the energy stored in the capacitor, the energy stored in the launch coil, and the kinetic energy of the plate.

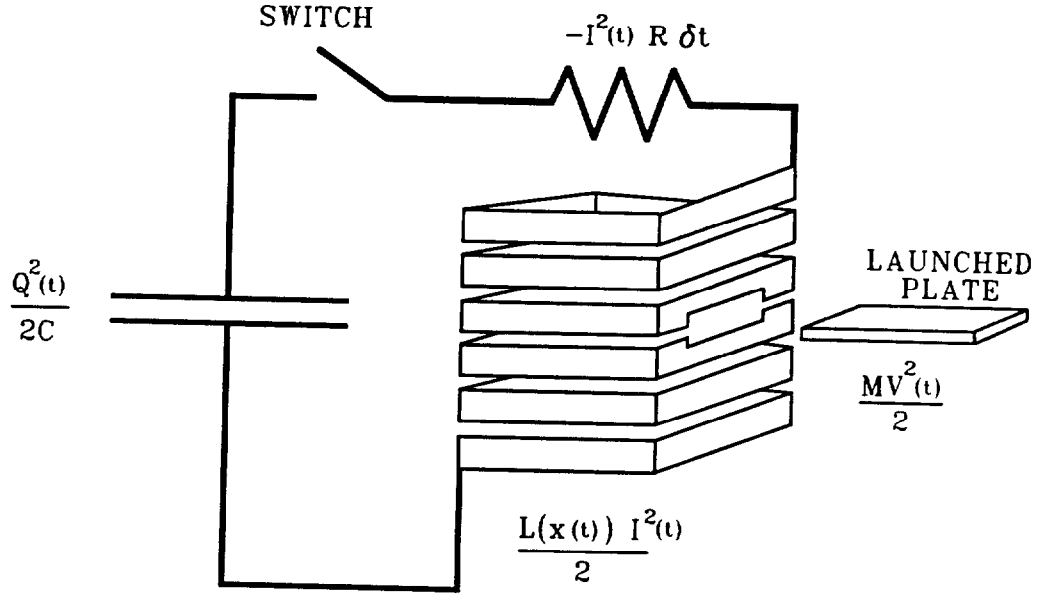

Figure 2. Schematic of a Single-Stage Reconnection Gun.

Now consider the total energy of the system at some later time, δt, when

$$E(t + \delta t) = Q^2(t + \delta t)/2C + L[x(t + \delta t)]I^2(t + \delta t)/2 + mv^2(t + \delta t)/2 \ . \qquad (2)$$

This total energy, $E(t+\delta t)$, is not equal to $E(t)$ because energy is lost in the heating of the components of the circuit and the metal plate. It is assumed that this energy loss during the time interval δt is equal to $R\, I^2(t)\, \delta t$ where R is the total resistance of the capacitor bank, the ignitron switch, launch coil, and some equivalent resistance of the plate. Thus,

$$-R\, I^2(t)\, \delta t = E(t + \delta t) - E(t) \quad . \tag{3}$$

Taking the limit as δt approaches zero gives

$$-R\, I^2 = Q/C\, dQ/dt + d(LI^2)/dt/2 + mv\, dv/dt \quad . \tag{4}$$

This equation is simplified by using the sum of voltages around the circuit loop,

$$Q/C - RI - d(LI)/dt = 0 \quad , \tag{5}$$

where the first, second, and third term are the voltages across the capacitor, the equivalent circuit resistance, and launch coil, respectively. Using the identity $I = -dQ/dt$ and Equation 5, and carrying out the time derivatives, Equation 4 reduces to

$$mv\, dv/dt = I^2\, dL/dt\, (1/2) \quad , \tag{6}$$

which is the equation of motion of the plate. Furthermore, since

$$dL/dt = dL/dx\, dx/dt = dL/dx\, v \quad ,$$

Equation 6 may be rewritten as

$$m\, dv/dt = I^2\, dL/dx\, (1/2) \quad . \tag{7}$$

The velocity and the position of the plate can be calculated from Equation 7, once the inductance gradient dL/dx is determined and the current through the coil is measured. The inductance gradient, dL/dx, can be determined from $L(x)$, which is the inductance of the coil as a function of the position of a stationary plate in the coil.

3. EXPERIMENTAL ARRANGEMENT

A launch coil was constructed from a 23-cm-long (10 x 10 cm^2) aluminum box with 3-mm-thick walls. The sides of the box were milled to form a square helical coil with nine turns. A coil with similar dimensions (Freeman 1988) was considered in a two-dimensional computational study of a reconnection gun. The coil is confined on the outside by a stack of 5-cm-thick G10 fiber glass rectangles, and on the inside by filling most of the core with fiber glass resin. The center part of the core is not filled so that a plate can be positioned inside the coil through a spacing between the windings (Figure 1). The plate is positioned before launch with its back-edge in contact with the backside of the coil.

The inductance of the present launch-coil was measured by a Hewlett Packard 4274A Multifrequency LRC Meter after the plate was positioned at several locations in the coil. The frequency of the LRC Meter was 2,000 Hz which is close to the ringing frequency of the circuit—2,200 Hz for the 1,670 μf capacitor bank. When the plate was placed in contact with the backside of the coil, the inductance was 2.052 μH. The inductance was 2.484 μH when the plate was halfway out and 2.726 μH when the plate was completely removed. Assuming that the inductance varies as a second-degree polynomial, then

$$L(x) = 2.052 + 10.54\,x - 38\,x^2 \tag{8}$$

and

$$dL(x)/dx = 10.54 - 76.0\,x \tag{9}$$

for $x < 0.10$ m, where 0.10 m is the width of the coil. This inductance gradient is used to calculate the final velocity for each plate launch considered in this report.

After a capacitor bank was charged to an initial voltage, the Ignitron switch (represented by the switch in Figure 1) was closed, connecting the capacitor bank (represented as a capacitor in Figure 1) to the coil and launching the plate. The velocity of the plate was then determined by two break wires mounted in the flight path of the plate and separated by 30 cm (not shown in Figure 1). This procedure was repeated for various metal plates and for various initial voltages on different capacitor banks. Three different capacitor banks with different total capacitances (1,670 μF, 1,040 μF, and 515 μF) were operated without a crowbar circuit,

allowing the circuit to ring. By changing the total capacitance, the ringing frequency of the circuit was changed as a test for frequency effects on the velocity of the plates. In a few launchings, the circuit was prevented from ringing by activating a crowbar circuit.

4. EXPERIMENTAL RESULTS

A total of 133 shots were conducted with the coil before it failed due to accumulated mechanical stresses. In 99 of these shots, the plate velocity was measured and grouped (see the Appendix) according to the material and mass of the plates and also the capacitance of the capacitor bank. These results and the results of other experiments where the velocity of the plate was not measured are discussed in this section.

4.1 Aluminum and Copper Plates. The analysis of the data from a particular plate launching is shown in detail as an example of the analysis performed on all the plates. In this shot, a 96-g aluminum plate was launched with a velocity of 250 m/s when a 1,670-μF capacitor bank was charged to 9,200 V. A Rogowski coil measured the time derivative of the coil current which was then integrated to determine the current through the coil (Figure 3). Using this current and the inductance gradient for the coil, the equation of motion was solved numerically to find the position (Figure 4) and the velocity of the plate (Figure 5) at any time.

The final velocity is reached at the time (0.524 ms in Figure 4) when the plate has travelled the width of the coil (0.10 m). According to Figure 5, the velocity at this time is 297.6 m/s. To make the comparison between the experimental and calculated velocities easier, an error is defined as

$$E = (Vt - Ve)/Ve \quad . \tag{10}$$

The error in this example is 0.19, where Vt is the calculated velocity (297.6 m/s) and Ve is the experimental velocity (250 m/s).

The average and the standard deviation of the errors for each group of copper and aluminum plates (Appendix A) are presented in Figure 6. The bars represent one standard deviation for each group. These results are plotted against the mass of the plate to show any

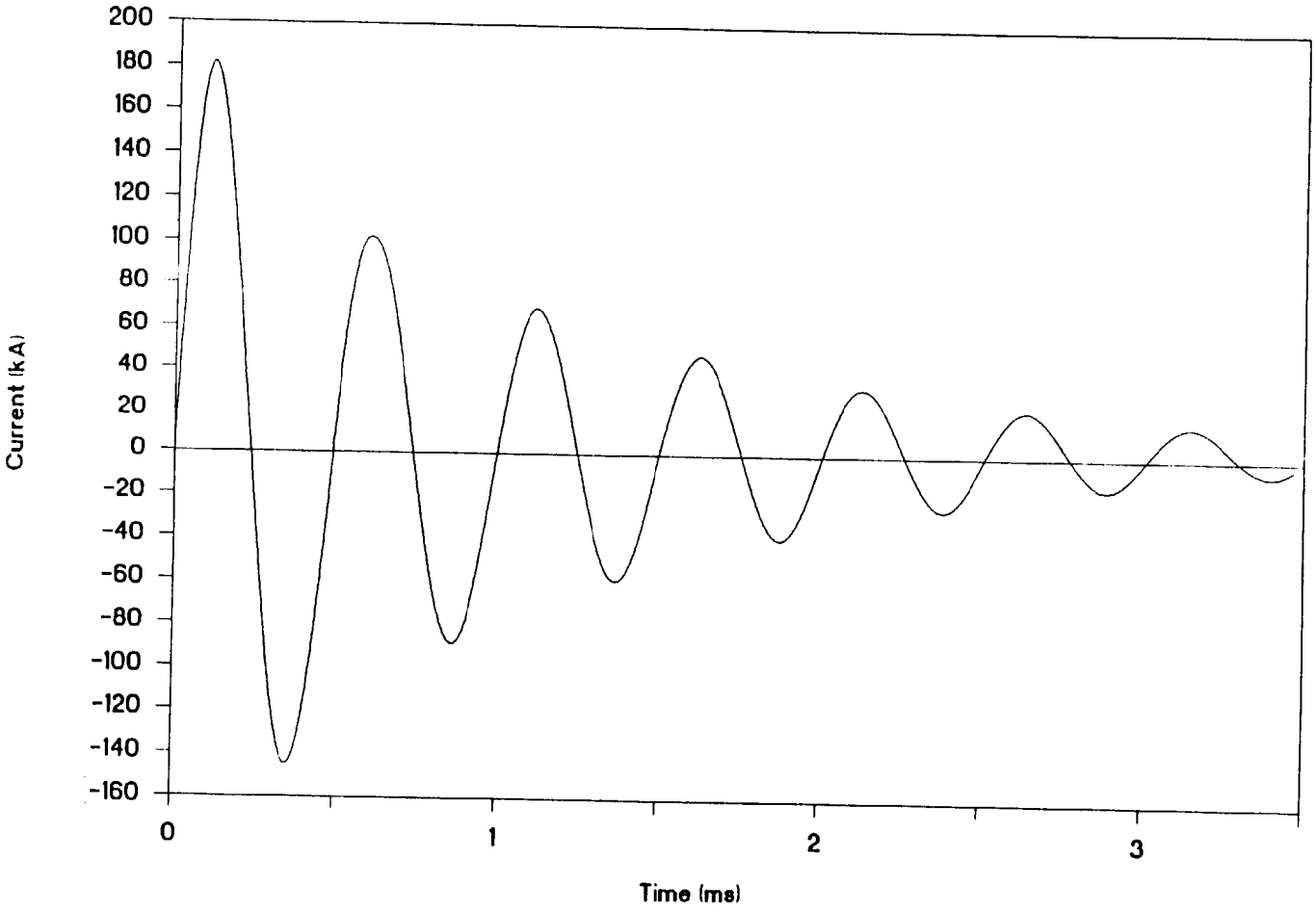

Figure 3. Current in the Reconnection Gun Circuit.

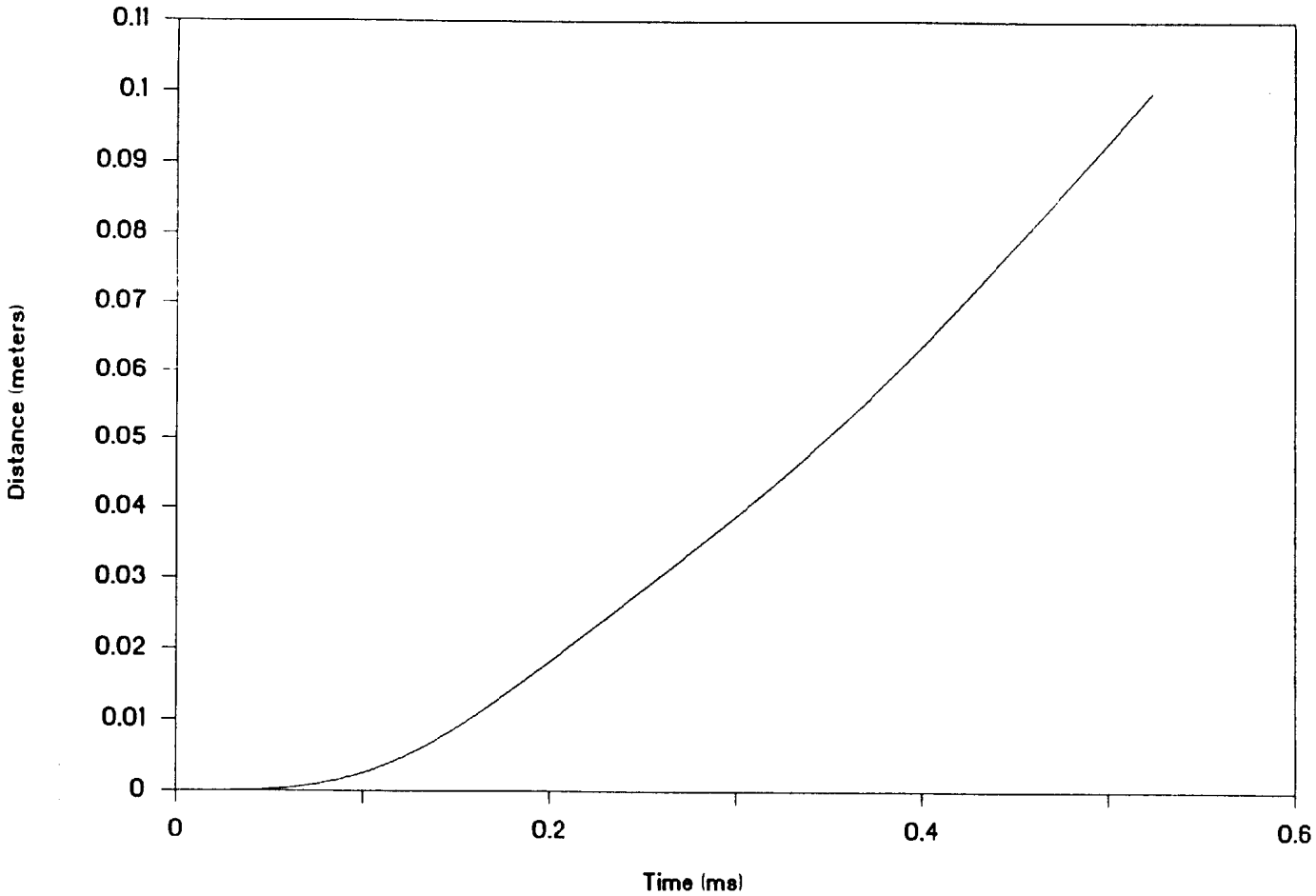

Figure 4. Position of an Aluminum Plate During Launch.

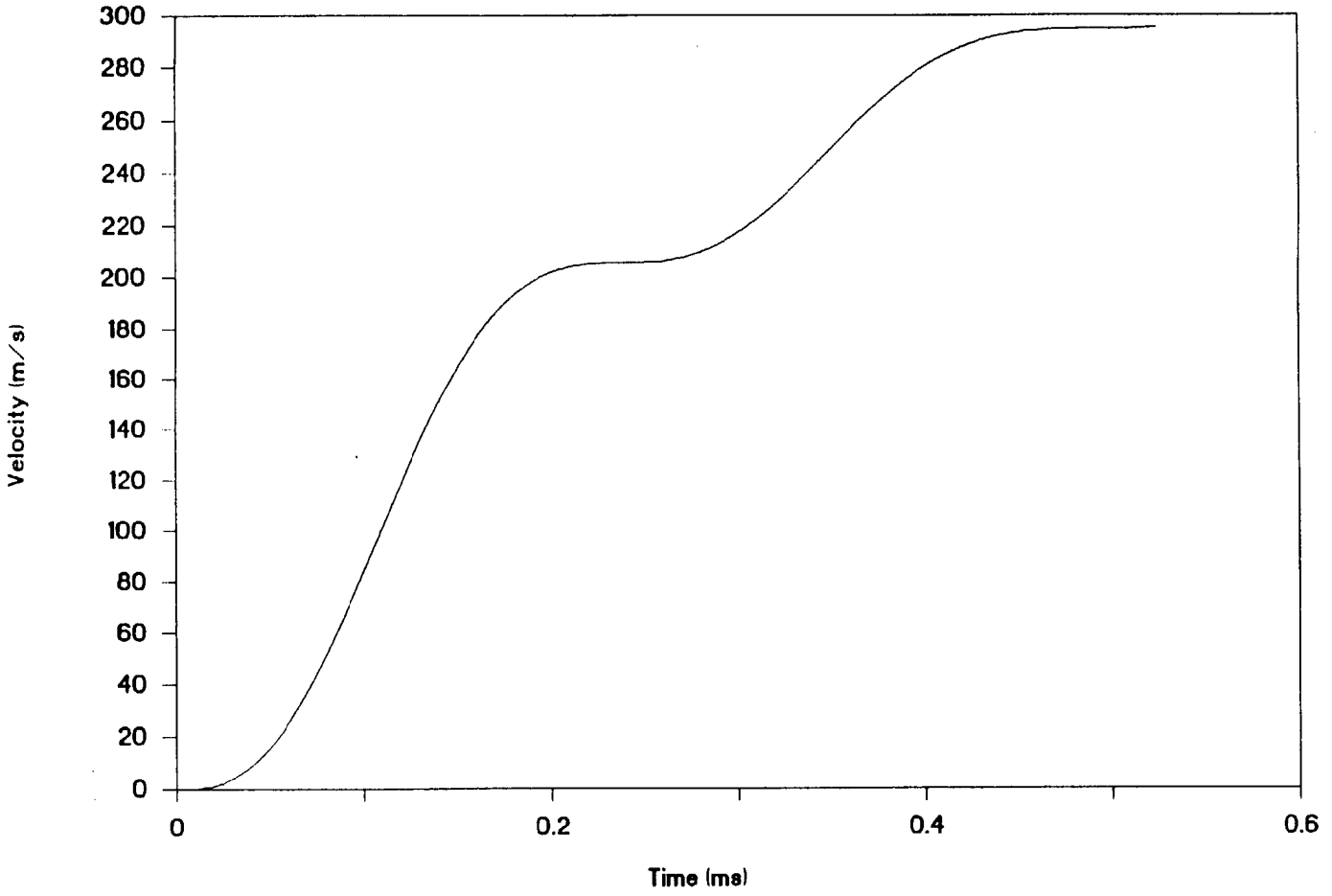

Figure 5. Velocity of an Aluminum Plate During Launch.

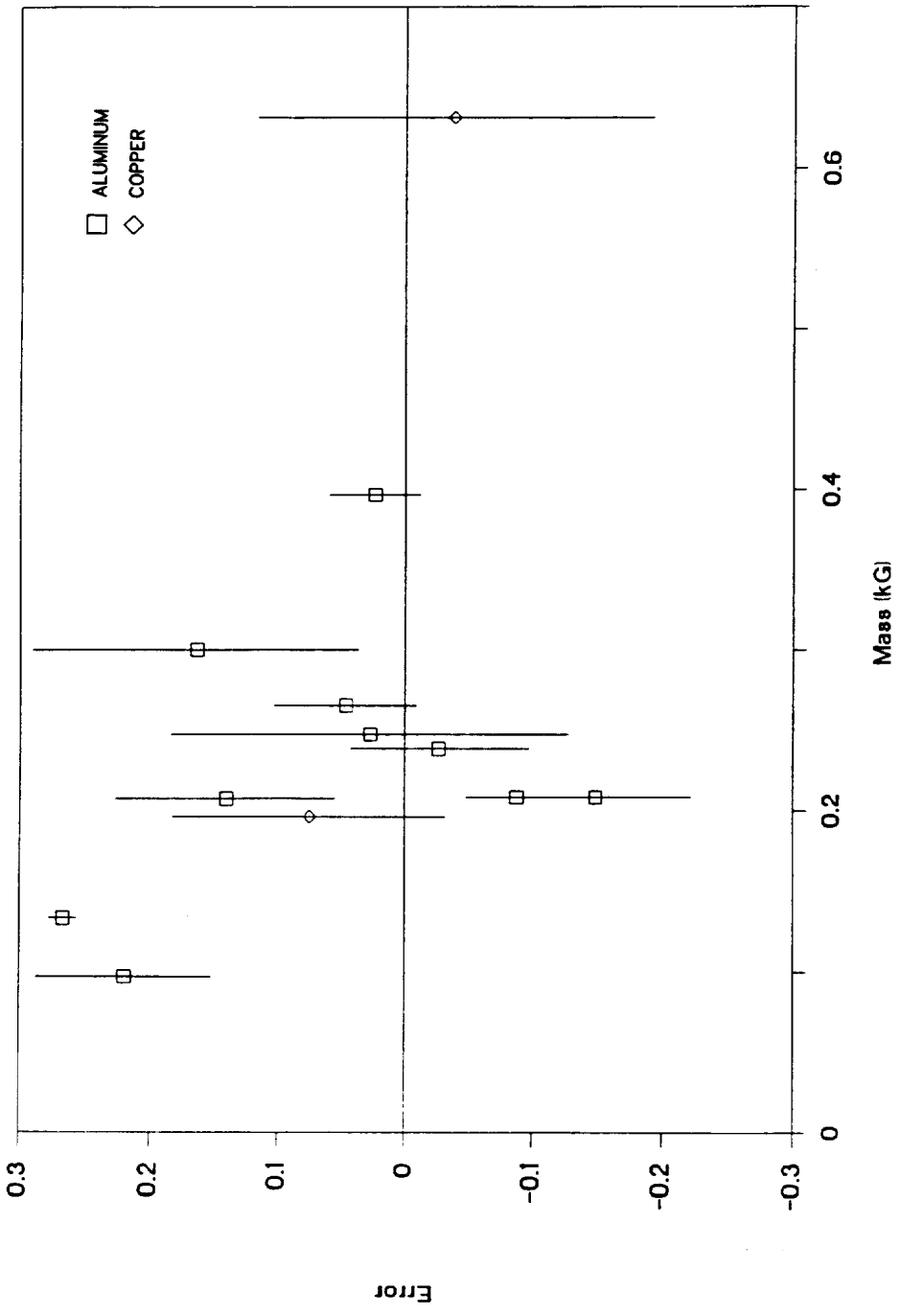

Figure 6. Errors for the Copper and Aluminum Plate Velocities.

trends that may depend on the mass of the plate. There is a possible decrease in the average errors as the mass increases that may be caused by plate heating, eddy currents in parts of the plate outside the coil, or some other effect not included in the equation of motion.

Although the equation of motion may not include all effects, it gives the final velocities within a maximum error of about 0.30 for a wide variety of masses, capacitor charges, and capacitor banks. Because the average for all the errors is 0.06, and the standard deviation for all the errors is 0.15, the equation of motion gave final velocities within an error ranging from −0.09 to +0.21 on average.

As stated before, the inductance of the launch coil was measured at 2,000 Hz, which is close to the ringing frequency of the circuit because the inductance of the launch coil depends on the frequency due to skin depth effects. Thus, this model indirectly includes skin depth effects through the inductance gradient. To test for skin depth effects, different capacitor banks were used to change the ringing frequency, and thus change the skin depth and the inductance gradient of the coil. Metal plates that had thicknesses on the order of the skin depth were also used as a test for skin depth effects. The model, however, predicts the velocities reasonably well for the different capacitor banks and over the entire range of plate thicknesses. Thus, skin depth effects are not obvious in this set of data. To provide some insight into these effects, the coil of the reconnection gun was driven by currents with different time profiles in an auxiliary experiment.

In this auxiliary experiment, the coil was driven by both underdamped current waveform and an overdamped current waveform. The Fourier transform of the underdamped current waveform shows a maximum at a high frequency whereas the transform for the overdamped case peaks at zero frequency. Because the skin depth is inversely proportional to the square root of the frequency (Knoepfel 1970), the effective skin depth for the underdamped current is much smaller than that for the overdamped current. The coil with an underdamped current waveform was obtained by operating the capacitor bank without a crowbar circuit. An overdamped current waveform was obtained by placing a crowbar switch in parallel with the launch coil. This produced a current that increased to a maximum as in the first quarter cycle of a sine wave and decayed exponentially after the crowbar switch was closed. These two very different current profiles were used to launch a 238-g aluminum plate with the same initial

charge voltage on the capacitor bank. The measured velocities of the plate for the underdamped current and the overdamped current are 44 m/s and 21 m/s, respectively. The model predicts velocities of 43.0 m/s for the underdamped current and 60.0 m/s for the overdamped current. Thus, the model failed badly when the overdamped current produced large skin depths.

4.2 Velocity vs. Time. The position of a plate during the launch was determined by optical means as another test of the model. A plate had two parallel rails that extended outside the coil when the plate was in its initial launch position. Mounted across these rails was a clear plastic sheet that had black bars printed on it which interrupted a light path. The time of interruption was recorded on a digital oscilloscope during the launch cycle. Thus, the position of the plate was recorded as a function of time which permitted determination of the plate velocity.

Figure 7 shows the experimental velocity as +, and the predicted velocity as a solid line. The consistency of the two curves show that the equation of motion can predict reasonably well the velocity of the plate at any time. The error, as defined by Equation 10 for the calculated velocity of 21 m/s and the experimental velocity of 19 m/s, is 0.10, which is well within the range of errors observed in other launchings.

4.3 Plate Heating in the Magnetic Field. The induced currents in the plate produce heating during the launch phase, while the plate resides within the magnetic field. Because these currents have a nonuniform distribution within the plate and on the surface, the surface temperature distribution should also be nonuniform immediately after launch. To observe a surface temperature distribution, an aluminum plate was fabricated with a nose section which held a nail oriented along the direction of plate motion. The nail was driven into a plywood barrier by the plate and stopped for viewing by an infrared 8–12 μm video camera immediately after launch. The aluminum plate had a thick anodized coating to increase the emissivity of the surface for the infrared radiation. The infrared video image (Figure 8) shows that the top surface of the plate was heated along its trailing and side edges where the magnetic field was concentrated.

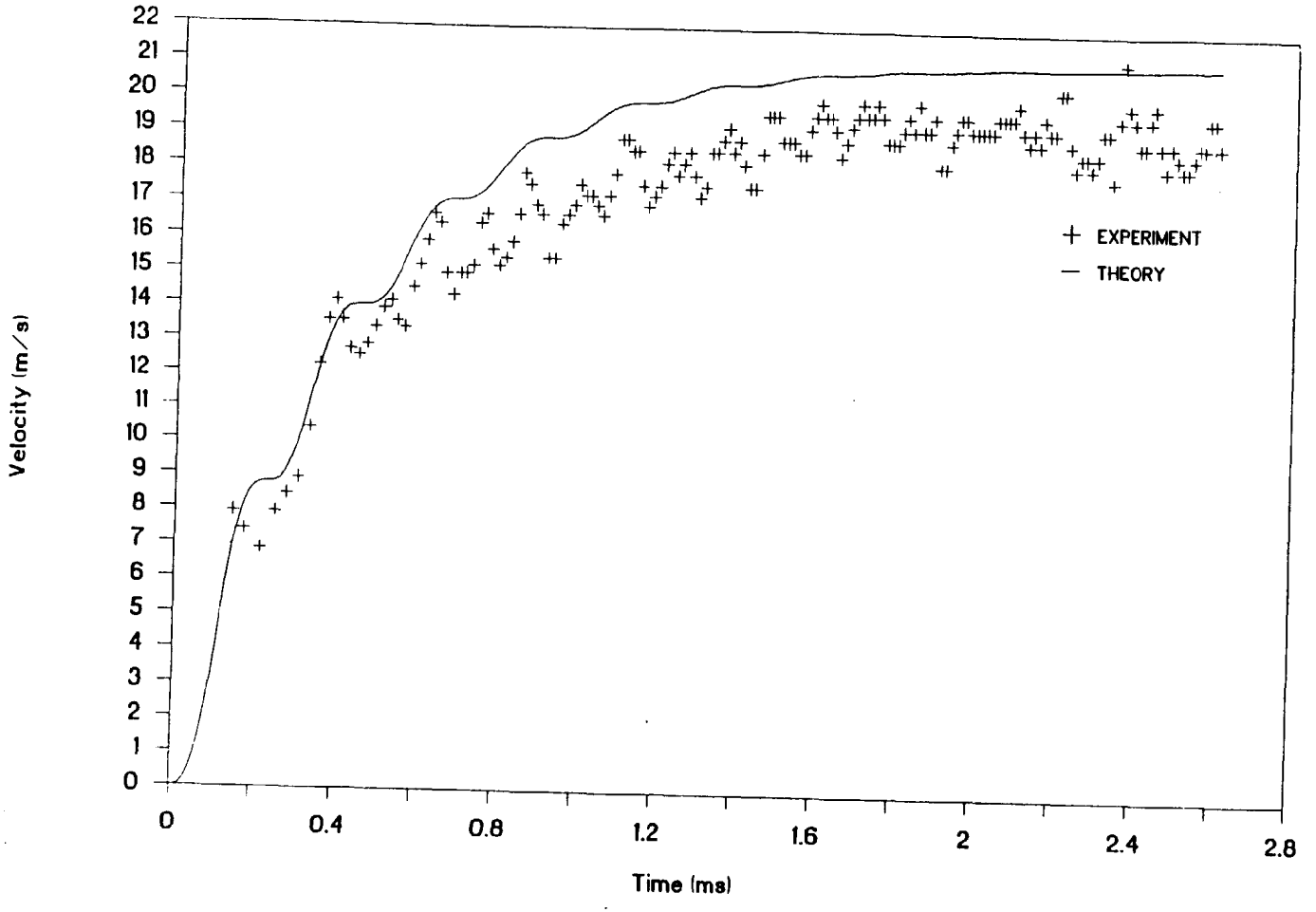

Figure 7. Experimental Velocity and Theoretical Velocity of an Aluminum Plate During Launch.

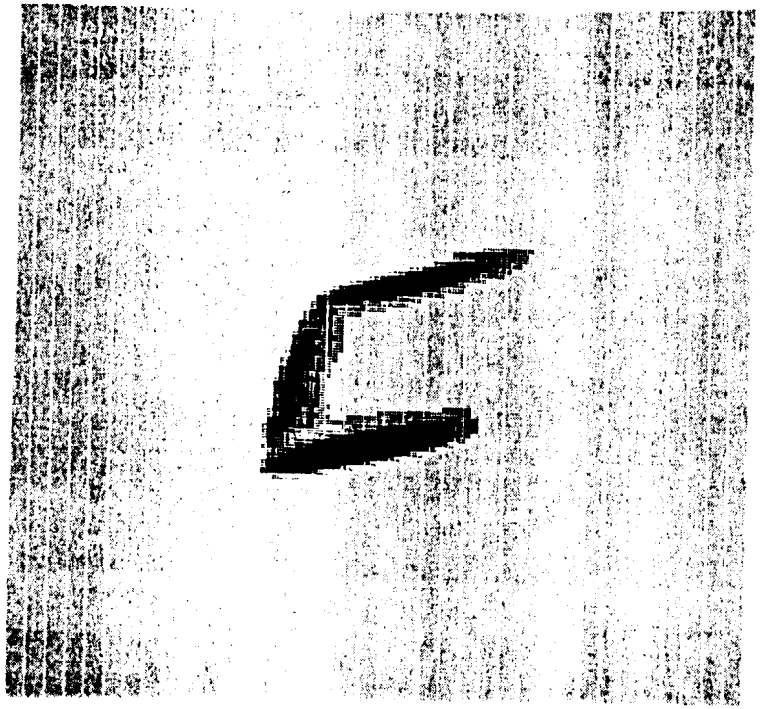

Figure 8. Infrared Image of an Aluminum Plate Just After Launching.

Figure 9 shows a selected horizontal video line signal which approximately bisects the trailing edge of the plate in the video image. The distance scale for this line was estimated by picking other features in this signal and correlating them to features with known distances, such as the length of the plate. This line shows that the heated region along the edges extends inward about 20 mm from the edges.

The data of Figure 9 show that little or no heating occurred in the middle of the plate, even though the thickness of the plate was about twice the skin depth. Thus, the magnetic field was effectively excluded from the volume as though it were a thick plate. Therefore, in our geometry, the thickness of a plate may not be the most important dimension to use to gauge the significance of skin depth effects. Plate length or plate width may be the more important indicator of these effects.

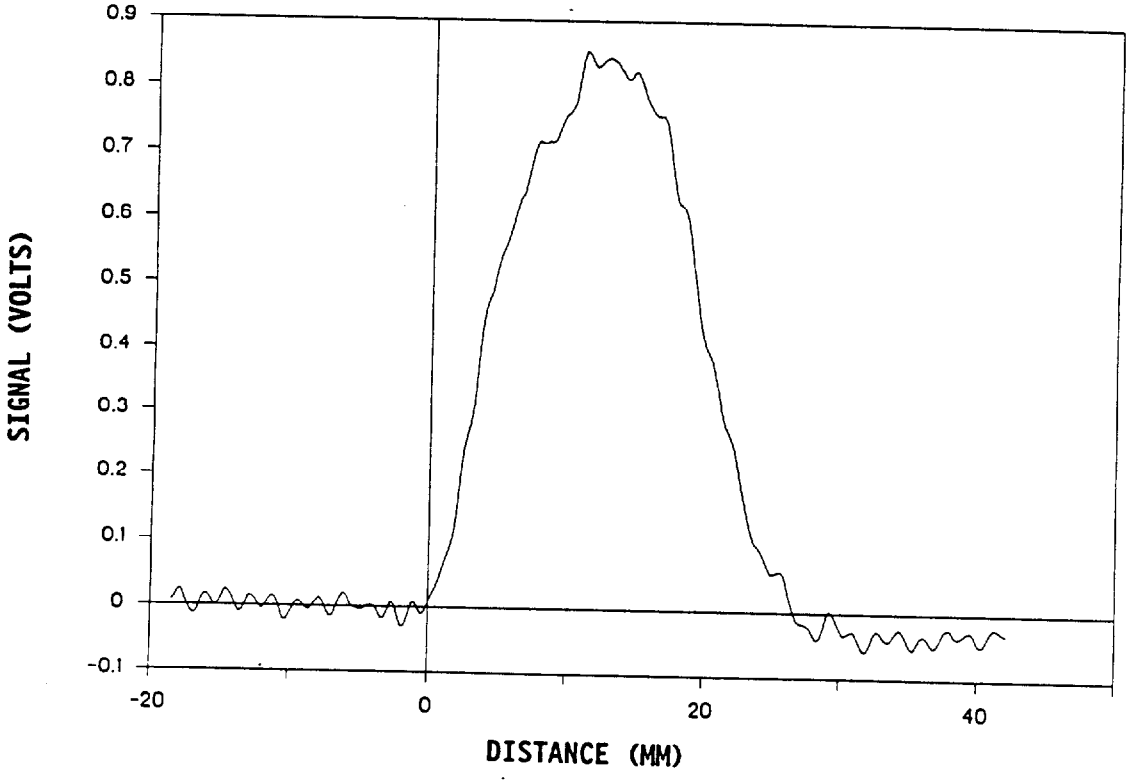

Figure 9. Infrared Intensity Distribution.

4.4 Results for Iron Plates. Instead of calculating an error for the velocities as was done for the Al and Cu data, the calculated velocity was divided by the experimental velocity for each shot. The velocities and their ratios for all the iron plates are grouped according to plate mass and capacitor bank (see Appendix B) in the same way as was done for the aluminum and copper results. The average and standard deviation of the ratios for each group (Figure 10) shows that the ratios are approximately equal within a group. Thus, the calculated velocities are proportional to the experimental velocities within that group. The ratios decrease as the mass of the plate increases or as the thickness of the plate increases (the iron plates all have the same length [13 cm] and width [8.5 cm]). This trend in the ratio may be due to the heating or the plate or to the magnetic properties of the iron, or other unknown factors. Therefore, the simple theory developed and tested in the present work is inadequate to explain the iron data. Further work is required in order to understand the interaction of iron plates with the magnetic field.

5. THE DESIGN OF A LAUNCH-COIL FOR FUTURE SYSTEMS

The first step in designing a launch system is to decide on plate material and dimensions. Next, one estimates, through inductance calculations, the inductance gradient for candidate designs. Because inductance is a geometrical property, simple models of the coils can be constructed from common laboratory materials and used to determine inductance values. Indeed, the initial model for a particular design, similar to the coil used in these experiments, was constructed from aluminum foil and cardboard. As the inductance measured for this coil model was in reasonable agreement with the estimated value, a more refined model was constructed using aluminum sheets riveted together. The inductance of each model was measured as a function of plate position within the coil (for an approximately one-quarter scale Al plate) for several locations in order to simulate the complete launch cycle. These data were then used to predict the currents delivered to the coil by various capacitor banks and, using the simple model, the final velocity of the plate. This procedure is currently being followed to design the coil for a 200-kJ reconnection gun.

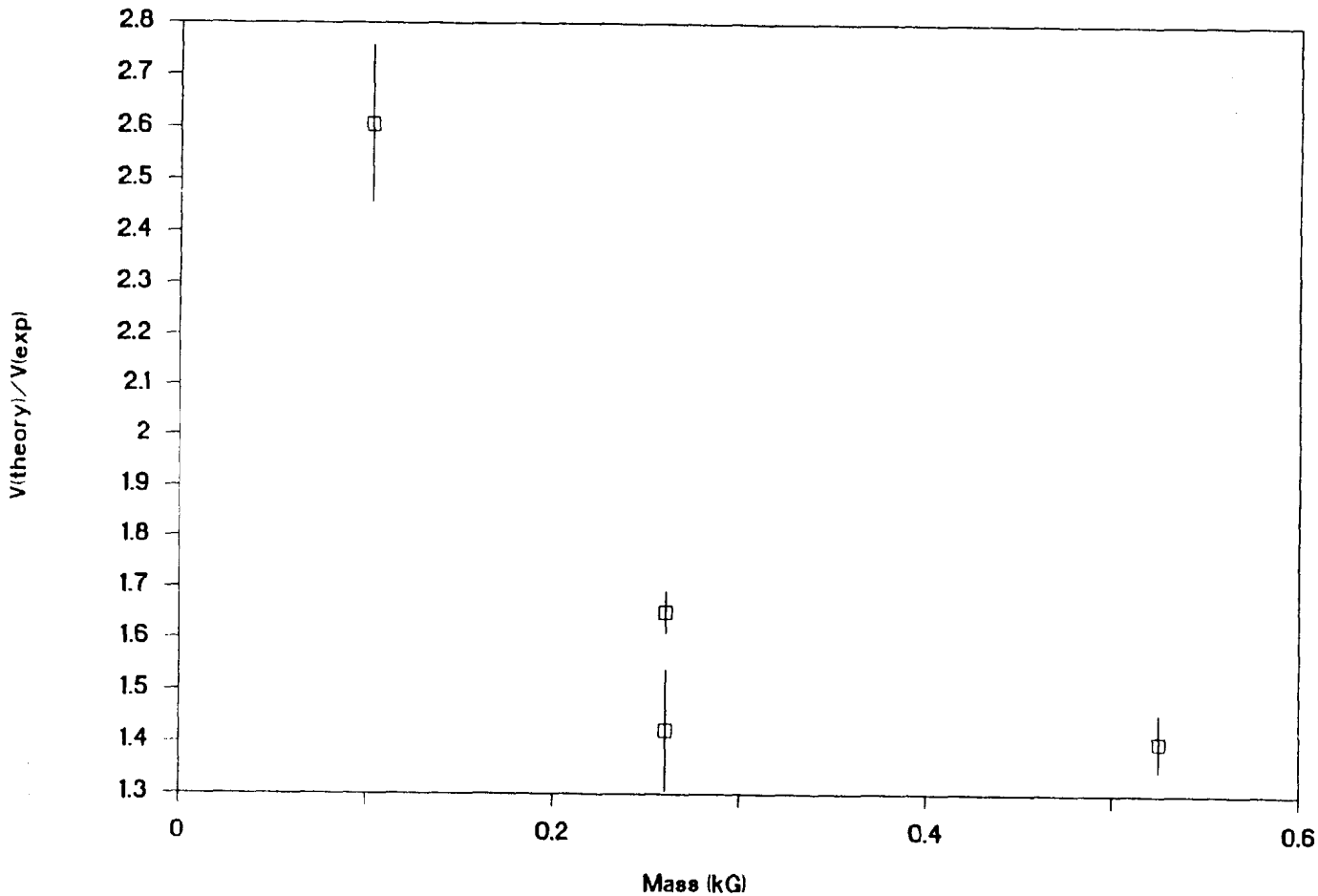

Figure 10. Velocity Ratios for Iron Plates.

6. CONCLUSION

A single-stage reconnection gun has been constructed and used to accelerate flat metal plates, oriented edge-on, to high velocities in a short distance. A 96-g plate was accelerated to a final velocity of 250 m/s in a distance of 10 cm, corresponding to an average acceleration of 32 kg's. A simple equation of motion which does not include the magnetic properties of the plate, heating, and other effects was used to predict the plate velocities. The equation of motion predicts velocities that are in reasonable agreement with the experimentally observed values to within an error range of –0.09 to +0.21 for a wide variety of experimental conditions. The model does not, however, provide reasonable estimates for the final velocities of the iron plates.

The plate velocity during the launch phase was measured for an aluminum plate and compared with the model predictions. The shape of the predicted curve of plate velocity vs. time agreed well with the experimentally observed trend.

Infrared images of a thin aluminum plate obtained immediately after launch showed that the plate was heated in a narrow region along the trailing edge and the side edges, where the magnetic field and induced current is large; however, most of the plate area was not heated significantly.

INTENTIONALLY LEFT BLANK.

7. REFERENCES

Cowan, M. PAT-APPL-7-034 354, Filed: 6 April 1987.

Cowan, M., E. C. Cnare, B. W. Duggin, R. J. Kaye, and T. J. Tucker. Proceedings of the 3rd Symposium on Electromagnetic Launch Technology. Austin, TX, 1986, also in IEEE, New York, pp. 25–30, 1986.

Cowan, M., M. M. Widner, E. C. Cnare, B. W. Duggin, R. J. Kaye, and J. R. Freeman. "Exploratory Development of the Reconnection Launcher 1986–1990." Proc. IEEE Trans. Magnetics, vol. 27, no. 1, pp. 563–567, January 1991.

Freeman, J. R. "REGGIE, A 2-D Reconnection Gun Code." Sandia Report SAND88-0518UC-28, Sandia National Laboratories, Albuquerque, NM, May 1988.

Frey, R. B., G. Melani, and S. R. Stegall, "Interactions Between Kinetic Energy Penetrators and Reactive Armor." BRL-TR-2964, U.S. Army Ballistic Research Laboratory, Aberdeen Proving Ground, MD, October 1988.

Hummer, C. R., and C. E. Hollandsworth. "Launching of Flat Plates With a Single Stage Reconnection Gun." Proceedings of the 8th IEEE International Pulsed Power Conference, IEEE Cat. No. 91CH3052-8, San Diego, CA, pp. 789, 16–19 June 1991.

Knoepfel, H. Pulsed High Magnetic Fields. New York, NY: North-Holland Publishing Co, 1970.

Prakash, A. Private communication. U.S. Army Ballistic Research Laboratory, Aberdeen Proving Ground, MD, January 1990.

Thomson, G. M., A. Prakash, D. Showalter, and P. Plostins. Private communication. U.S. Army Ballistic Research Laboratory, Aberdeen Proving Ground, MD, January 1991.

INTENTIONALLY LEFT BLANK.

APPENDIX A:

DATA FOR COPPER AND ALUMINUM PLATES

INTENTIONALLY LEFT BLANK.

Table A-1. Aluminum (96 g), 1,670-μF Capacitor Bank

V (volts)	Ve (m/s)	Vt (m/s)	Error
1,500	9.8	11.2	0.14
2,000	17.6	21.0	0.19
2,500	25.7	33.5	0.30
3,000	42.4	47.9	0.13
3,500	52.2	62.2	0.19
3,500	52.6	65.3	0.24
4,000	68.0	79.2	0.16
4,500	81.2	96.5	0.19
5,000	93.2	124.4	0.33
5,000	102.5	119.1	0.16
6,500	139.2	179.1	0.29
7,500	176.0	232.8	0.32
9,200	250.0	297.6	0.19
			Average Error = 0.22 ± 0.07

Table A-2. Aluminum (133 g), 1,670-μF Capacitor Bank

V (volts)	Ve (m/s)	Vt (m/s)	Error
2,500	20.3	25.5	0.26
5,000	72.7	92.9	0.28
			Average Error = 0.27 ± 0.01

Table A-3. Aluminum (206 g), 1,670-μF Capacitor Bank

V (volts)	Ve (m/s)	Vt (m/s)	Error
3,000	23.2	24.9	0.07
3,500	26.1	33.0	0.26
3,500	30.7	31.2	0.02
3,500	31.9	34.0	0.07
4,000	39.9	46.8	0.17
4,500	48.9	51.2	0.05
5,000	55.0	63.0	0.15
6,500	90.5	104.1	0.15
7,500	107.5	128.4	0.19
9,000	132.6	169.8	0.28
			Average Error = 0.14 ± 0.09

Table A-4. Aluminum (238 g), 1,670-μF Capacitor Bank

V (volts)	Ve (m/s)	Vt (m/s)	Error
2,500	8.7	8.1	−0.07
2,500	9.1	8.7	−0.04
2,500	9.3	8.5	−0.09
5,000	44.0	48.1	0.09
			Average Error = −0.03 ± 0.07

Table A-5. Aluminum (247 g), 1,670-μF Capacitor Bank

V (volts)	Ve (m/s)	Vt (m/s)	Error
2,500	8.6	7.5	−0.13
2,500	12.0	14.2	0.18
			Average Error = 0.03 ± 0.16

Table A-6. Aluminum (265 g), 1,670-μF Capacitor Bank

V (volts)	Ve (m/s)	Vt (m/s)	Error
2,500	8.1	8.6	0.06
2,500	8.3	8.8	0.06
2,500	10.1	9.4	-0.07
3,500	18.0	19.1	0.06
3,500	17.0	18.2	0.07
3,500	17.7	20.0	0.13
3,500	17.9	18.2	0.02
			Average Error = 0.05 ± 0.06

Table A-7. Aluminum (300 g), 1,670-μF Capacitor Bank

V (volts)	Ve (m/s)	Vt (m/s)	Error
2,500	13.1	13.8	0.05
3,000	17.4	21.3	0.22
3,500	22.4	21.2	-0.05
3,500	25.9	29.2	0.13
4,000	26.8	36.7	0.37
4,400	32.0	39.8	0.24
5,000	43.0	50.8	0.18
			Average Error = 0.16 ± 0.13

Table A-8. Aluminum (396 g), 1,670-μF Capacitor Bank

V (volts)	Ve (m/s)	Vt (m/s)	Error
3,000	12.3	12.2	-0.01
3,500	15.9	16.0	0.01
3,500	17.1	17.5	0.02
4,000	20.5	22.6	0.10
4,500	27.0	27.1	0.00
5,000	33.4	34.0	0.02
			Average Error = 0.02 ± 0.04

Table A-9. Aluminum (208 g), 1,040-μF Capacitor Bank

V (volts)	Ve (m/s)	Vt (m/s)	Error
2,500	7.5	5.5	–0.27
3,000	9.8	8.1	–0.17
3,500	14.1	11.4	–0.19
4,000	18.0	14.7	–0.18
4,500	24.0	19.7	–0.18
5,000	31.1	25.8	–0.17
5,500	32.7	29.7	–0.09
6,000	36.6	36.5	–0.00
6,500	48.9	45.0	–0.08
Average Error = 0.15 ± 0.07			

Table A-10. Aluminum (208 g), 515-μF Capacitor Bank

V (volts)	Ve (m/s)	Vt (m/s)	Error
3,500	5.5	4.7	–0.15
5,000	11.7	10.5	–0.10
6,000	17.3	16.3	–0.06
6,950	24.8	23.7	–0.04
Average Error = –0.09 ± 0.04			

Table A-11. Copper (631 g), 1,670-μF Capacitor Bank

V (volts)	Ve (m/s)	Vt (m/s)	Error
3,500	11.6	9.4	–0.19
4,000	14.6	13.3	–0.09
4,500	17.6	14.4	–0.18
5,000	20.6	23.8	0.16
5,000	22.0	17.3	–0.21
7,500	47.7	52.6	0.10
9,000	62.9	72.2	0.15
Average Error = –0.04 ± 0.16			

Table A-12. Copper (196 g), 1,040-μF Capacitor Bank

V (volts)	Ve (m/s)	Vt (m/s)	Error
3,000	9.9	9.6	−0.03
4,000	18.1	18.9	0.04
5,000	30.1	31.1	0.03
6,000	38.9	48.8	0.25
			Average Error = 0.08 ± 0.11

INTENTIONALLY LEFT BLANK.

APPENDIX B:

DATA FOR IRON PLATES

INTENTIONALLY LEFT BLANK.

Table B-1. Iron (103 g), 1,670-μF Capacitor Bank

V (volts)	Ve (m/s)	Vt (m/s)	Vt/Ve
2,000	7.0	16.8	2.40
2,500	10.3	26.0	2.52
3,000	15.6	38.1	2.44
3,500	20.4	53.6	2.63
4,000	24.2	69.5	2.87
4,500	32.8	86.7	2.64
5,000	36.5	99.6	2.73
			Average = 2.61 ± 0.15

Table B-2. Iron (260 g), 1,670-μF Capacitor Bank

V (volts)	Ve (m/s)	Vt (m/s)	Vt/Ve
2,500	7.2	11.8	1.64
3,000	10.5	17.7	1.69
3,500	14.8	24.7	1.67
4,000	20.1	31.8	1.58
4,500	22.8	38.9	1.71
5,000	28.6	46.5	1.63
			Average = 1.65 ± 0.04

Table B-3. Iron (525 g), 1,670-μF Capacitor Bank

V (volts)	Ve (m/s)	Vt (m/s)	Vt/Ve
3,500	8.0	11.1	1.39
4,000	10.8	15.4	1.43
4,500	13.2	19.5	1.48
5,000	17.8	23.5	1.32
			Average = 1.40 ± 0.06

Table B-4. Iron (260 g), 1,040-μF Capacitor Bank

V (volts)	Ve (m/s)	Vt (m/s)	Vt/Ve
3,500	6.6	8.5	1.29
4,000	8.3	11.2	1.35
4,500	10.3	14.5	1.41
5,000	13.0	18.7	1.44
6,000	17.0	27.8	1.64
		Average =	1.42 ± 0.12

No. of Copies	Organization
2	Administrator Defense Technical Info Center ATTN: DTIC-DDA Cameron Station Alexandria, VA 22304-6145
1	Commander U.S. Army Materiel Command ATTN: AMCAM 5001 Eisenhower Ave. Alexandria, VA 22333-0001
1	Director U.S. Army Research Laboratory ATTN: AMSRL-D 2800 Powder Mill Rd. Adelphi, MD 20783-1145
1	Director U.S. Army Research Laboratory ATTN: AMSRL-OP-CI-A, Tech Publishing 2800 Powder Mill Rd. Adelphi, MD 20783-1145
2	Commander U.S. Army Armament Research, Development, and Engineering Center ATTN: SMCAR-IMI-I Picatinny Arsenal, NJ 07806-5000
2	Commander U.S. Army Armament Research, Development, and Engineering Center ATTN: SMCAR-TDC Picatinny Arsenal, NJ 07806-5000
1	Director Benet Weapons Laboratory U.S. Army Armament Research, Development, and Engineering Center ATTN: SMCAR-CCB-TL Watervliet, NY 12189-4050
(Unclass. only)1	Commander U.S. Army Rock Island Arsenal ATTN: SMCRI-TL/Technical Library Rock Island, IL 61299-5000
1	Director U.S. Army Aviation Research and Technology Activity ATTN: SAVRT-R (Library) M/S 219-3 Ames Research Center Moffett Field, CA 94035-1000

No. of Copies	Organization
1	Commander U.S. Army Missile Command ATTN: AMSMI-RD-CS-R (DOC) Redstone Arsenal, AL 35898-5010
1	Commander U.S. Army Tank-Automotive Command ATTN: ASQNC-TAC-DIT (Technical Information Center) Warren, MI 48397-5000
1	Director U.S. Army TRADOC Analysis Command ATTN: ATRC-WSR White Sands Missile Range, NM 88002-5502
1	Commandant U.S. Army Field Artillery School ATTN: ATSF-CSI Ft. Sill, OK 73503-5000
(Class. only)1	Commandant U.S. Army Infantry School ATTN: ATSH-CD (Security Mgr.) Fort Benning, GA 31905-5660
(Unclass. only)1	Commandant U.S. Army Infantry School ATTN: ATSH-CD-CSO-OR Fort Benning, GA 31905-5660
1	WL/MNOI Eglin AFB, FL 32542-5000
	Aberdeen Proving Ground
2	Dir, USAMSAA ATTN: AMXSY-D AMXSY-MP, H. Cohen
1	Cdr, USATECOM ATTN: AMSTE-TC
1	Dir, ERDEC ATTN: SCBRD-RT
1	Cdr, CBDA ATTN: AMSCB-CI
1	Dir, USARL ATTN: AMSRL-SL-I
10	Dir, USARL ATTN: AMSRL-OP-CI-B (Tech Lib)

No. of
Copies Organization

1 Director
Defense Advanced Research
Projects Agency
ATTN: Dr. Peter Kemmey
3701 North Fairfax Dr.
Arlington, VA 22203-1714

1 Commander
SDIO
ATTN: SDIO/IST,
MAJ M. Huebschman
Washington, DC 20301-7100

2 Commander
U.S. Army Armament Research,
Development, and Engineering Center
ATTN: SMCAR-FSA-E,
Dr. T. Gora
John Bennett
Picatinny Arsenal, NJ 07806-5000

1 Commander
U.S. Army Armament Research,
Development, and Engineering Center
ATTN: SMCAR-AEE-B,
Dr. D. Downs
Picatinny Arsenal, NJ 07806-5000

2 Commander
U.S. Army Armament Research,
Development, and Engineering Center
ATTN: SMCAR-CCL-FA,
H. Moore
H. Kahn
Picatinny Arsenal, NJ 07806-5000

2 Director
Benet Weapons Laboratory
U.S. Army Armament Research,
Development, and Engineering Center
ATTN: SMCAR-CCB-DS,
Dr. C. A. Andrade
SMCAR-CCB-RM,
Dr. Pat Vottis
Watervliet, NY 12189

No. of
Copies Organization

1 Director
U.S. Army Research Office
ATTN: Dr. Michael Ciftan
P. O. Box 12211
Research Triangle Park, NC 27709-2211

2 Commander
U.S. Army Electronics Technology and
Devices Laboratory
Pulse Power Technology Branch
ATTN: SLCET-ML, Dr. Thomas Podlesak
SLCAT-P, Dr. Hardev Singh
Fort Monmouth, NJ 07703

1 Commander
U.S. Navy David Taylor Research Center
Code 1740.3
ATTN: Dr. Ray Garrison
Bethesda, MD 20084

4 CG, MCRDAC
Code AWT
ATTN: Dr. C. Vaughn
Mr. C. Childers
MAJ R. Jensen
Mr. G. Solhand
Quantico, VA 22134-5080

2 Air Force Armament Laboratory
ATTN: AFATL/DLJG,
Mr. Kenneth Cobb
AFATL/DLDG,
Dr. T. Aden
Eglin AFB, FL 32542-5000

1 Director
Brookhaven National Laboratory
ATTN: Dr. J. R. Powell
Bldg 129
Upton, NY 11973

1 Director
Lawrence Livermore National Laboratory
ATTN: Dr. R. S. Hawke, L-156
P. O. Box 808
Livermore, CA 94550

No. of Copies Organization

3 Director
Los Alamos National Laboratory
ATTN: MSG 787,
Mr. Max Fowler
Dr. J. V. Parker
Dr. William Condit
Los Alamos, NM 87545

1 Director
Sandia National Laboratories
ATTN: Dr. Maynard Cowan
Dept. 1220
P. O. Box 5800
Albuquerque, NM 87185

1 NASA Lewis Research Center
ATTN: MS 501-7, Lynette Zana
2100 Brook Park Road
Cleveland, OH 44135

2 Auburn University
ATTN: Dr. Raymond F. Askew,
Leach Nuclear Science Center
Dr. E. J. Clothiaux,
Department of Physics
Auburn University, AL 36849-3501

1 Texas Tech University
Department of EE
ATTN: Dr. M. Kristiansen
P.O. Box 43102
Lubbock, TX 79409-3102

1 Tuskegee Institute
Dept. of Mechanical Engineering
ATTN: Dr. Pradosh Ray
Tuskegee Institute, AL 36088

1 University of Alabama in Huntsville
School of Science & Engineering
ATTN: Dr. C. H. Chen
Huntsville, AL 35899

1 University of Miami
ATTN: Dr. Manuel A. Huerta,
Physics Dept.
P.O. Box 248046
Coral Gables, FL 33124

No. of Copies Organization

1 University of Tennessee
Space Institute
ATTN: Dr. Dennis Keefer
Tullahoma, TN 37388-8897

2 University of Texas
Center for Electromechanics
Balcones Research Center
ATTN: Mr. William Weldon
Mr. Raymond Zaworka
10100 Burnet Road, Bldg. 133
Austin, TX 78748

1 Institute for Advanced Technology
ATTN: Dr. Harry Fair
4030-2 W. Braker Lane
Austin, TX 78759

1 Southwest Research Institute
ATTN: Dr. David Littlefield
P.O. Box 28510
6220 Culebra Road
San Antonio, TX 78228-0510

3 Maxwell Laboratories
ATTN: Dr. Rolf Dethlefson
Dr. Ian McNab
Dr. Mark Wilkinson
8888 Balboa Avenue
San Diego, CA 92123

1 California Research and
Technology, Inc.
Titan Technologies
ATTN: Dr. Richard F. Johnson
20943 Devonshire Street
Chatsworth, CA 91311-2376

1 Boeing Aerospace Company
ATTN: Dr. J. E. Shrader
P. O. Box 3999
Seattle, WA 98134

2 GA Technologies, Inc.
ATTN: Dr. Robert Bourque
Dr. L. Holland
P. O. Box 85608
San Diego, CA 92138

No. of
Copies Organization

2 Electromagnetic Research, Inc.
ATTN: Dr. Henry Kolm
Dr. Peter Mongeau
2 Fox Road
Hudson, MA 01749

2 General Electric Company (AEPD)
ATTN: Dr. William Bird
Dr. Slade L. Carr
R. D. #3, Plains Road
Ballston Spa, NY 12020

1 General Research Corporation
ATTN: Dr. William Isbell
P. O. Box 6770
Santa Barbara, CA 93160-6770

2 IAP Research, Inc.
ATTN: Dr. John P. Barber
Mr. David P. Bauer
2763 Culver Avenue
Dayton, OH 45429-3723

2 LTV Aerospace & Defense Company
ATTN: MS TH-83,
Dr. Michael M. Tower
Dr. C. H. Haight
P. O. Box 650003
Dallas, TX 75265-0003

1 Pacific-Sierra Research Corp.
ATTN: Dr. Gene E. McClellan
1401 Wilson Blvd.
Arlington, VA 22209

1 Science Applications International Corporation
ATTN: Dr. K. A. Jamison
1247-B North Eglin Parkway
Shalimar, FL 32579

3 Science Applications International Corporation
ATTN: Dr. Jad H. Batteh
Dr. G. Rolader
Mr. L. Thornhill
1503 Johnson Ferry Road, Suite 100
Marietta, GA 30062

No. of
Copies Organization

1 System Planning Corporation
ATTN: Donald E. Shaw
1500 Wilson Blvd.
Arlington, VA 22209

2 Westinghouse Science and Technology Center
ATTN: Dr. Bruce Swanson
Mr. Doug Fikse
1310 Beulah Road
Pittsburgh, PA 15233

1 Dr. E. W. Sucov
1065 Lyndhurst Drive
Pittsburgh, PA 15206

2 SPARTA Inc.
ATTN: Jeffery Kezerian
Dr. Michael M. Holland
9455 Towne Centre Drive
San Diego, CA 92121-1964

1 Supercon Inc.
ATTN: Charles Renaud
830 Boston Turnpike Road
Shrewsbury, MA 01545

Aberdeen Proving Ground

1 Cdr, USATECOM
ATTN: AMSTE-SI-F

USER EVALUATION SHEET/CHANGE OF ADDRESS

This Laboratory undertakes a continuing effort to improve the quality of the reports it publishes. Your comments/answers to the items/questions below will aid us in our efforts.

1. ARL Report Number **ARL-TR-14** Date of Report **November 1992**

2. Date Report Received _____

3. Does this report satisfy a need? (Comment on purpose, related project, or other area of interest for which the report will be used.) _____

4. Specifically, how is the report being used? (Information source, design data, procedure, source of ideas, etc.) _____

5. Has the information in this report led to any quantitative savings as far as man-hours or dollars saved, operating costs avoided, or efficiencies achieved, etc? If so, please elaborate. _____

6. General Comments. What do you think should be changed to improve future reports? (Indicate changes to organization, technical content, format, etc.) _____

CURRENT ADDRESS

_____
Organization

_____
Name

_____
Street or P.O. Box No.

_____
City, State, Zip Code

7. If indicating a Change of Address or Address Correction, please provide the Current or Correct address above and the Old or Incorrect address below.

OLD ADDRESS

_____
Organization

_____
Name

_____
Street or P.O. Box No.

_____
City, State, Zip Code

(Remove this sheet, fold as indicated, staple or tape closed, and mail.)

DEPARTMENT OF THE ARMY

OFFICIAL BUSINESS

BUSINESS REPLY MAIL
FIRST CLASS PERMIT No 0001, APG, MD

Postage will be paid by addressee

Director
U.S. Army Research Laboratory
ATTN: AMSRL-OP-CI-B (Tech Lib)
Aberdeen Proving Ground, MD 21005-5066

NO POSTAGE
NECESSARY
IF MAILED
IN THE
UNITED STATES